From tissue phenotype to proteotype: Sensitive protein identification in microdissected tumor tissue

ZHENGPING ZHUANG[1], STEVE HUANG[1], JEFF A. KOWALAK[2], YING SHI[3], JINGQI LEI[4], MAKOTO FURUTA[1], YOUN-SOO LEE[1], IRINA A. LUBENSKY[1], GRIFFIN P. RODGERS[3], ALBERT S. CORNELIUS[5], ROBERT J. WEIL[1], BIN T. TEH[6] and ALEXANDER O. VORTMEYER[1]

[1]Surgical Neurology Branch, NINDS/NIH, [2]Mass Spectrometry Laboratory, NIMH/NIH; [3]Molecular and Clinical Hematology Branch, NIDDK/NIH, 10 Center Drive, Bethesda, MD 20892; [4]Transmedix Corporation, 9700 Great Seneca Highway, Rockville, MD 20850; [5]Division of Pediatric Hematology/Oncology, DeVos Children's Hospital, 100 Michigan NE, Grand Rapids; [6]Laboratory of Cancer Genetics, Van Andel Research Institute, 333 Bostwick Avenue NE, Grand Rapids, MI 49503, USA

Received September 19, 2005; Accepted October 24, 2005

Abstract. Correlation of disease phenotype with protein profile (proteotype) is a significant challenge for biomedical research. The main obstacles have been the need to insure sufficient quantities of pure protein sample, the reproducibility of protein display, and rapid and accurate protein identification. We present a modified approach that combines enhanced detection sensitivity with tissue microdissection from frozen primary renal cancer tissues of different histological subtypes, followed by 2D gel analysis and protein identification with MALDI mass spectrometry. We obtained reliable and highly consistent results in phenotypically similar tumors of each individual subtype by performing strict morphological control of the analyzed tumor cells without physical or chemical alteration of the frozen tissue samples. By application of non-oxidizing silver staining, proteins were resolved and identified with high levels of specificity and sensitivity. This new combination of techniques allows not only for sensitive identification of specific protein patterns that correspond to a histological tumor phenotype, but also for identification of specific disease-associated protein targets.

Introduction

Proteomic analysis is being used increasingly to identify potential protein targets and biomarkers in serum or plasma (1-3), urine (4,5), CSF (3), and saliva (3,6). Tumor tissues represent a rich source of distinct proteins that may closer characterize the biology of tumor development. These proteins can be correlated with various clinico-pathological features, including diagnosis, prognosis, and drug response. In addition, they may represent novel therapeutic targets. To obtain more complete proteotypic spectra of tumors, however, tumor tissue itself needs to be subjected to proteomic analysis. Principally, any tumor tissue can be screened by various high throughput proteomic techniques. However, tumor tissue removed at surgery not only consists of neoplastic cells, but a large number of diverse 'normal' cells including vascular cells, fibrous cells, and inflammatory cells. Without careful histological evaluation, attempts to isolate 'tumor' and 'normal' tissue from surgical specimens are of limited value, as the exact nature of the cells is unknown at the time of gross tissue procurement. In addition to various immunological, vascular and fibroproliferative responses, the tumor itself may exhibit considerable intratumoral variability in regard to tumor cell biology. For example, when malignant tumor growth is not accompanied by sufficient neovascularization, subsets of tumor cells may undergo pathways of hypoxic stress response and finally apoptosis and/or necrosis. Therefore, results may differ significantly even among tissue samples obtained from the same tumor.

Careful selection of tumor cells, preceded by light-microscopic visualization of stained tissue sections, is therefore essential to permit an accurate and reproducible comparison of the proteotypes among different tumors. In the past, the major disadvantage of tissue sections for histological control of tumor tissue analysis has been 2-fold: First, histological control is performed on 10-μm thick sections from which only small amounts of tissue can be recovered by microdissection. Second, histological tissue sections need to be stained with dyes, the chemical nature of which may substantially interfere with subsequent protein analysis (7-9).

We report here an effective and reproducible combination of approaches to obtain proteotypic profiles of primary renal tumor tissue under strict morphological control. We chose to study renal tumors because they are known to be histologically

Correspondence to: Dr Alexander O. Vortmeyer, NINDS/National Institute of Health, 10 Center Drive, Bldg 10, Rm 4N242, Bethesda, MD 20892, USA
E-mail: vortmeyera@ninds.nih.gov

Key words: proteomics, RCC, profiling

heterogenous and can be correlated with distinct chromosomal and molecular profiles. Our approaches are essentially based on selective dissection of fresh frozen tumors after careful histological analysis of stained serial sections, followed by 2D gel analysis, enhanced sensitivity gel staining, and subsequent MALDI spectrometry for protein identification. It is concluded from our results that individual types of tumors are associated with specific proteotypic profiles. Individual protein spots can be excised and sequenced by MS/MS, either for diagnostic confirmation or for identification of potential new biomarkers or therapeutic targets.

Materials and methods

Tissue. A series of human kidney tumors was collected with IRB approval by the Van Andel Research Institute, Michigan, and from the Cooperative Human Tissue Network (CHTN). Surgically procured tumor tissue was evaluated by a pathologist, and any tumor parts that were relevant for tissue diagnosis were processed separately for diagnostic evaluation. Additional tumor tissue was kept either frozen or in formalin for experimental studies.

A series of primary renal tumors was used including clear cell renal cell carcinoma (ccRCC, n=3), papillary carcinoma (PC, n=3), oncocytoma (OC, n=3), and Wilms' tumor (WT, n=3). ccRCC, PC, OC, and WT are histologically distinct types of renal cancer with well-defined, characteristic morphological features (10). Of each tumor, parts were frozen at the time of surgical resection for possible subsequent experimental analysis; other parts were fixed in formalin and embedded in paraffin for tumor classification. Only tumors with an unequivocal histological diagnosis (ccRCC, n=3; PC, n=3; OC, n=3; WT, n=3) were considered for further proteomic analysis. From the tumors with unequivocal histopathological diagnosis, a single 10-μm frozen section was taken and stained with hematoxylin and eosin for special histological evaluation. A semiquantitative cell count was performed on tumor-rich areas that were uncompromised by inflammation, necrosis, or reactive fibrosis; subsequently, these areas would be subjected to selective tumor dissection from serial sections from the same block. The primary goal was to obtain 100,000 viable tumor cells, which were obtained from 1 to 10 consecutive sections taken from the selected blocks. Procurement of normal kidney tissue, or areas of inflammation, necrosis or hemorrhage, was strictly avoided. Tissue dissection was performed manually, as described previously (11), to avoid possible heating artifacts induced by laser-assisted technology (7,8,12,13). However, unstained serial sections were used to avoid chemical artifacts induced by tissue staining (14).

Two dimensional SDS PAGE. Dissected tissue, with an estimated 100,000 cells, was collected into 30 μl of extraction buffer II containing 8 M urea, 4% (w/v) CHAPS, 40 mM Tris, 0.2% (w/v) Bio-Lyte 3/10, and 2 mM tributyl phosphine (Bio-Rad, Hercules, CA), vigorously vortexed at room temperature for 60 min, and centrifuged in a microcentrifuge at 12,000 RPM for 15 min. The supernatant was combined with 150 μl of rehydration buffer (Bio-Rad) containing 8 M urea, 2% CHAPS, 50 mM DTT, and 0.2% (w/v) Bio-Lyte 3/10 ampholytes, before isoelectric focusing.

The first dimension of 2D electrophoresis was performed on a Protean IEF System (Bio-Rad) with ReadyStrip IPG strips (pH 4-7, 11 cm, Bio-Rad) rehydrated with 185 μl of sample for 12 h and subsequently subjected to high voltages at 20˚C for electric focusing: 250 V for 20 min, 8000 V for 2 h and 30 min, and a final step of 25000 V/h. IPG strips were washed in rehydration buffer I containing 6 M urea, 2% SDS, 375 mM Tris-HCl (pH 8.8), 20% glycerol, and 2% (w/v) DTT; and buffer II containing 6 M urea, 2% SDS, 375 mM Tris-HCl (pH 8.8), 20% glycerol, and 2.5% (w/v) iodoacetamide (Bio-Rad), for 10 min each. Criterion Precast Gels (8-16% Tris-HCl, 1.0 mm) (Bio-Rad) were used for the second dimension of protein separation in a Criterion Dodeca cell (Bio-Rad) under a constant voltage of 200 V for 55 min. Gels were stained with Bio-Rad's Silver Stain Plus kit (Bio-Rad). The staining procedure is based on the methods developed by Gottlieb and Chavko (15), in which no oxidization of proteins takes place, and silver ions transfer from tunstosillic acid to the proteins in the gel by means of an ion exchange or electrophilic process. Methanol and acetic acid needed for fixing gels were purchased from Sigma-Aldrich (St. Louis, MO).

In-gel digestion. Protein spots of interest were excised from the gel, placed into clean 0.5 ml Eppendorf tubes and stored at -20˚C. Silver-stained spots were destained according to Blum *et al* (16). After destaining, individual protein gel spots were subjected to reduction and alkylation, followed by *in situ* digestion with trypsin (17). The resultant peptide mixtures were recovered by sequential extraction (17), dried to near completion in a vacuum centrifuge, and diluted to a final volume of 10 μl in 5% CH_3CN, 0.1% HCO_2H.

Mass spectrometry. Peptides from in-gel digests were analyzed by capillary LC-MS/MS. An LC10VP series HPLC system (Shimadzu Scientific Instruments, Inc., Columbia, MD.) was interfaced to an LCQ ion trap mass spectrometer (Thermo-Finnigan, San Jose, CA). Reversed phase HPLC was carried out using a PicoFrit microbore column (0.075x100 mm; New Objective Inc., Woburn, MA) packed with 10 cm of BetaBasic 18 resin (Thermo Hypersil-Keystone, Bellefonte, PA) installed on a New Objective PicoView mounting system. The HPLC system was operated at 15 μl min^{-1} and the flow was split to ~200 nl min^{-1} using a 1000-psi back pressure regulator (Upchurch Scientific, Oak Harbor, WA). Mobile phase A was H_2O:CH_3CN:HCO_2H (94.9:5:0.1), while mobile phase B was H_2O:CH_3CN:HCO_2H (19.9:80:0.1). The chromatograph was developed using a linear gradient from 10% B to 60% B over 40 min. The LCQ was set to iteratively acquire a full MS scan between 400 and 1800 m/z followed by full MS/MS scans of the five most abundant ions from the preceding MS scan. Relative collision energy for collision-induced dissociation was set to 35% with a 30-ms activation time. Dynamic exclusion was enabled with a repeat count of 2, a repeat duration of 0.5 min, and a 1-min exclusion duration window.

Protein identification. Unprocessed data files containing MS/MS spectra were submitted to the Mascot search engine (MatrixScience Ltd., London, UK) for database searching using the Mascot daemon. Mascot compares the mass values

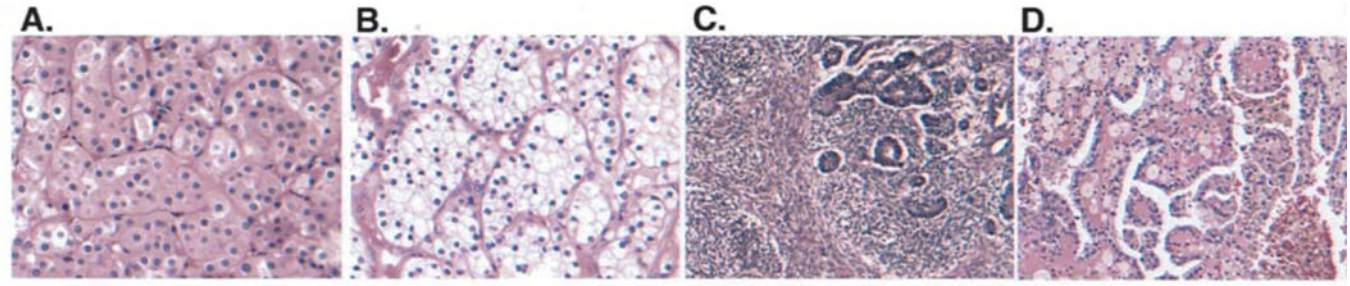

Figure 1. Four different tumor types with markedly distinct histopathological phenotypes were selected for the study. (A) Renal oncocytoma consists of cells with abundant, granular and eosinophilic cytoplasm that are tightly packed in solid nests; the nuclei are regular and round with no or small nucleoli. (B) Clear cell carcinoma is characterized by an alveolar architectural pattern with nests of cells separated by thin-walled vascular septae. (C) Wilms' tumor shows a triphasic pattern and contains blastemal, stromal, and epithelial cell types of differentiation. (D) Papillary carcinoma is composed of fibrovascular stalks filled with abundant lipid-laden macrophages and lined by neoplastic cells.

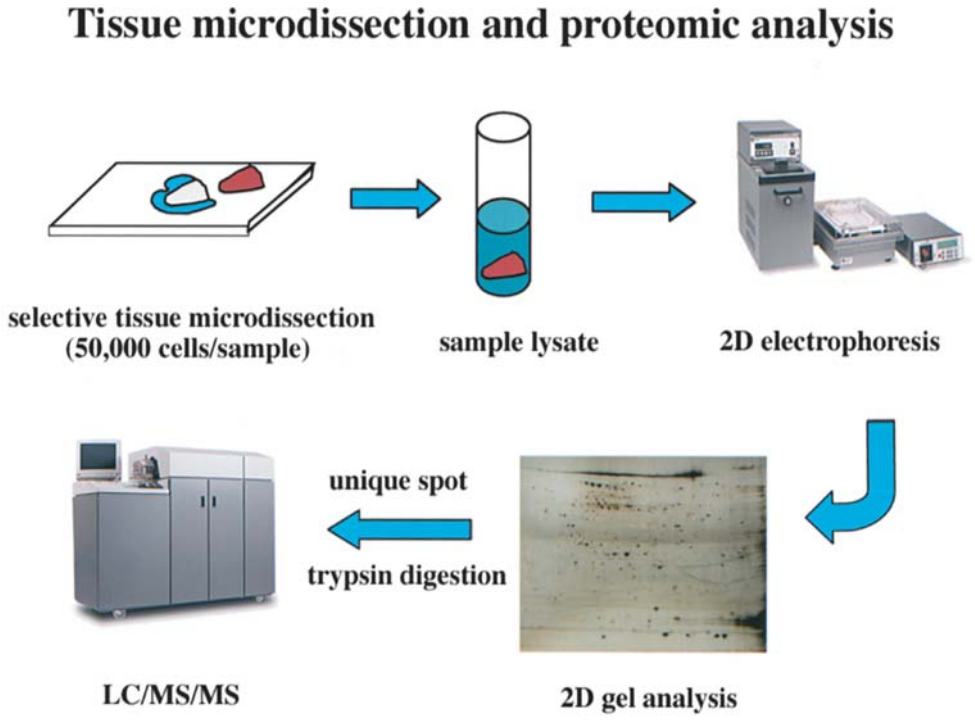

Figure 2. Tissue microdissection and proteomic analysis. After dissection of areas of interest, protein is extracted and subjected to 2D gel electrophoresis. Protein spots of interest are removed from the gel and analyzed by capillary LC/MS/MS.

of observed product ions with the mass values calculated for theoretical product ions from peptide sequences present in a specified genomic database. From this comparison, a probability-based score is calculated which reflects the statistical significance of the match between the product ion spectrum and the sequences contained in a database (18). The SwissProt-Trmbl database (19) was searched using *homo sapiens* as a taxonomic restrictor. Two statistically significant, unique peptides were considered to be the minimum for a positive identification as each peptide constitutes independent verification of the identified protein. While it is conceptually possible to identify a protein based on a single peptide, we considered single peptide identification as insufficient for protein identification due to the 'golden match standard'. Briefly, it is possible that a peptide sequence is deemed to be correct (i.e., the top match) based on statistical and/or subjective criteria but is not actually correct due to the incompleteness of genomic databases (20).

Statistical analyses. As the data were nonparametric, probability analyses were used to evaluate the likelihood of the outcome that one (or more) protein was expressed in one renal tumor subtype and not others. The probability that a protein was found in all of one tumor subtype but not in tumors of a second type, or *vice versa*, was calculated using the Mann-Whitney test. For a given protein, the Mann-Whitney test calculates the probability that a protein would split perfectly between the two groups. The calculated p-value was 0.001166. Given that there were an estimated 250 proteins found on each gel, it is likely that at least one protein would show a perfect split between the two types. If there is no other expected difference in any of the 250 proteins, the probability of at least one

protein randomly showing a perfect split between two groups is calculated in the following manner: $(1\text{-}0.001166)^{250}$, or 0.747015. Using the binomial distribution function, the likelihood that ≥10 proteins would be uniquely expressed in one subtype or the other [i.e. the probability that the 10 out of 250 proteins identified in papillary carcinomas (see Results) will discriminate perfectly] is given by binomial probability distribution, which in this case equals approximately $\geq 1 \times 10^{-9}$. These probabilities were generated under the assumption that protein expression levels are independent of one another, which, while not likely to be precisely true, does permit an estimation of the likelihood that the unique protein expression patterns in one subtype of kidney tumor or the other appear randomly. It does not take into account the additional variation introduced when comparing more than two tumor types in which proteins are expressed by only one tumor type and not any of the other two or three, which would probably increase the likelihood that these expression patterns are statistically significant.

Results

Four different types of renal tumor, clear cell carcinoma, papillary carcinoma, oncocytoma, and Wilms' tumor, were studied (Fig. 1). For all tumors, histopathological diagnosis was confirmed on regularly processed, formalin-fixed material. Additional frozen tumor samples were used for dissection and subsequent 2D-PAGE (Fig. 2).

Analysis of the different tumor types by 2D-PAGE revealed individual proteotypic profiles for clear cell carcinoma, papillary carcinoma, oncocytoma, and Wilms' tumor, respectively, as defined by the presence of individual proteins in one type of tumor but not in any other type of tumor or in normal kidney (Fig. 3). At the same time, analysis of different tumors of the same type derived from different patients revealed near-identical results (Fig. 4). Therefore, analysis of 12 renal tumors strongly suggests that each tumor type is associated with a specific 2D PAGE proteotype.

Each tumor sample obtained from the same type of renal tumor revealed 'differentially-expressed' protein spots that were absent in other types of renal tumor (Fig. 5 and Table I). Differentially expressed spots were excised from the 2D gel and subjected to spectrometric analysis. In clear cell carcinoma, spectrometric analysis of selected protein spots revealed members of the annexin and fibrinogen families of proteins (C1, C2, C3), cathepsin D preprotein (C4), α enolase (C5), proteasome activator subunit 1 (C6), glutathione transferase omega (C7), and ß2 tubulin (C8). In papillary carcinoma, we selectively identified NADH dehydrogenase FeS protein (P1), dehydrolipoamide succinyltransferase (P2), Annexin A2 (P3), phosphotriesterase-related protein (P4), annexin I (P5), an actin filament capping protein (P6), lamin A precursor (P7), γ enolase (P8), ß actin (P9), and α tubulin (P10). Proteins specific for Wilms' tumor included Ariadne-2 protein homolog (W1), zinc finger protein 267 (W2), makorin 1 (W3), a Krueppel-related zinc finger protein (W4), and Golgi-apparatus protein 1 precursor (W5). In renal oncocytoma, we selectively detected metallothioneins 1A and 1L (O1 and O3), copper transport protein ATOX1 (O2), and pyruvate dehydrogenase E1 component, ß (O4).

Discussion

After application of a combination of morphological and technical procedures to evaluate and process a variety of tumor tissues we conclude that individual types of renal tumor correspond to a specific, highly reproducible and individual proteotypic distribution of proteins (proteotype). Spectrometric analysis of differentially-expressed proteins revealed specific groups of proteins to be associated with the individual tumor types.

The applied combination of techniques therefore allow for accurate, consistent, and reproducible protein display using frozen tissue samples that are fully morphologically controlled. It is predominantly based on a tissue preservation technique that not only preserves integrity of protein, DNA and RNA, but also maintains morphological integrity. Preservation of morphology allows identification of areas of interest within frozen tissue samples that are free of normal tissue and of possible changes, such as necrosis, inflammation and hemorrhage, that may influence the results. Finally, preservation of morphology allows for semiquantitative assessments of cell counts to predict the number of sections that need to be obtained for tissue dissection from glass slides.

Protein was extracted according to standard protocols. Ampholytes with a pK range between 3 and 10 in conjunction with IPG strips pH 4.0-7.0 were used for initial separation of proteins to obtain the largest possible number of proteins; other pK ranges can be used if desired. Also, different protein extraction protocols would facilitate the identification of proteins of lesser solubility, e.g. membrane proteins. Specific extraction protocols, however, did not significantly increase the number of detected proteins and we speculate that thin-sectioning on a cryostat produces a significant mechanical effect on the tissue cells resulting in significantly increased extraction efficiency.

There are two principal ways for proteomic display of biological samples to obtain 'expression signatures'. Direct mass spectrometry has the advantage of a relatively complete display of low molecular weight fragments (<20 kDa) which are presumed to: i) be peptides, and ii) be representative of the entire proteome. The disadvantage of direct mass spectroscopy is the presence of abundant, non-specific signal, or 'noise', which needs to be reduced by multiple control analyses and complex statistical procedures. We chose the second approach; initial protein display by 2D-PAGE, followed by protein identification using tandem mass spectrometry. While the 2D-PAGE approach has lower sensitivity compared to direct mass spectrometry, it has proven to provide specific proteotypic profiles for individual pathological processes that are relatively free of non-specific signals. 2D PAGE-based proteomics has the advantage of spatial resolution of protein isoforms, e.g. two different annexin A2 isoforms were observed in clear cell carcinoma (C1) and papillary carcinoma (P3). Protein isoforms arise from differential transcription, post-translational modification, proteolytic processing, or combinations thereof, and the importance of the ability to resolve isoforms becomes magnified as one proceeds from qualitative to quantitative proteomics.

After obtaining specific expression profiles, we took further advantage of the 2D-PAGE approach by dissecting

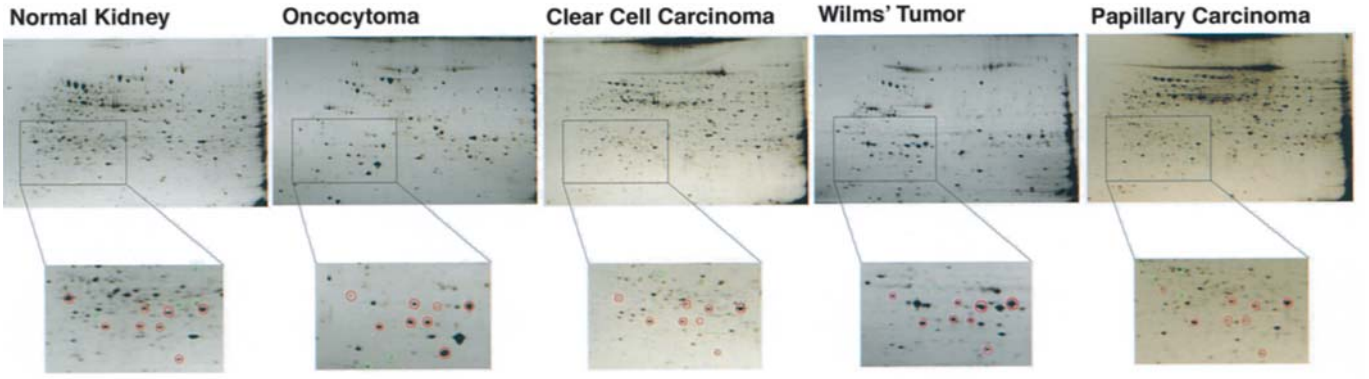

Figure 3. 2D PAGE analysis reveals individual proteotypic profiles for oncocytoma, clear cell carcinoma, Wilms' tumor, and papillary carcinoma. In the magnified areas, red circles indicate proteins that are consistently present in all types of tumors. Green circles indicate proteins that are differentially expressed in individual tumor types.

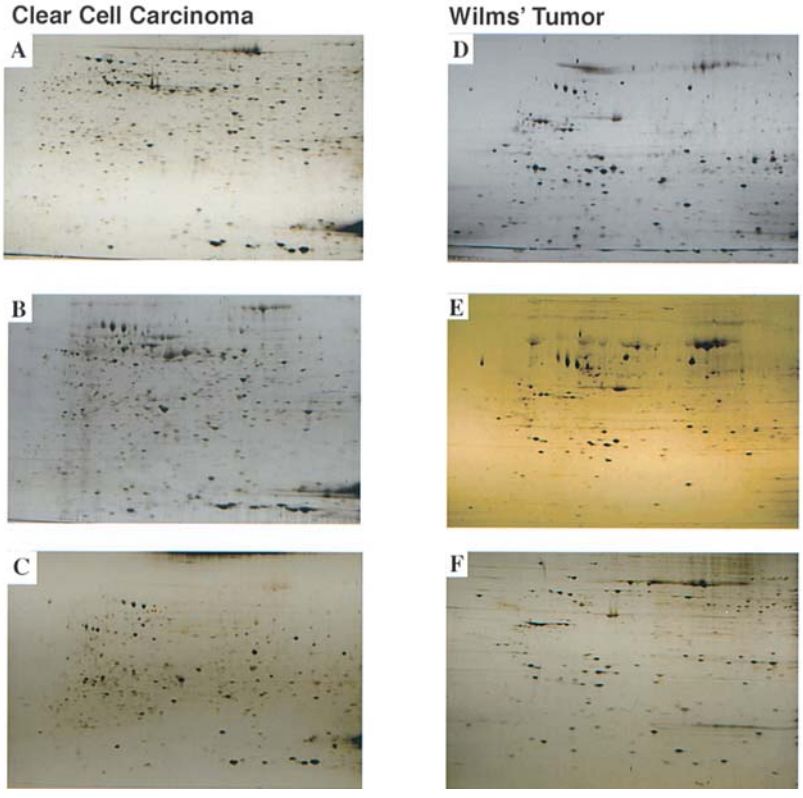

Figure 4. Different tumors of the same histopathologic phenotype show highly consistent proteotypic profiles after 2D PAGE analysis. A, B, and C show 2D gels of three different clear cell carcinomas; D, E, and F show 2D gels of three different Wilms' tumors.

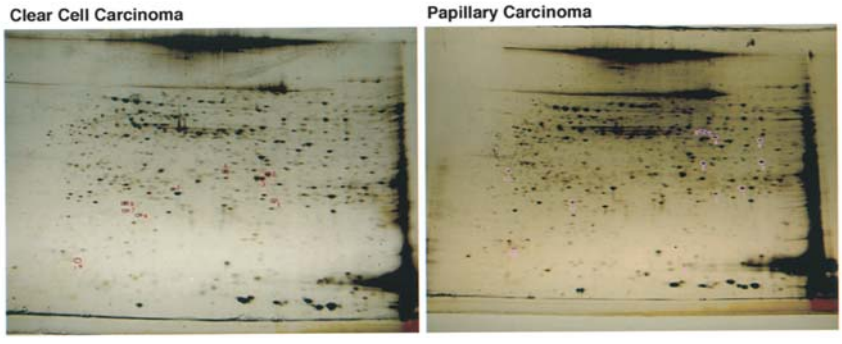

Figure 5. Differentially expressed proteins in clear cell carcinoma (left) versus papillary carcinoma (right) that were selected for protein identification. From clear cell carcinoma, spots 1-9 (corresponding to C1-C9 in Table I) were separately excised, destained, digested and analyzed by capillary LC-MS/MS. Similarly, spots 1-12 were analyzed from papillary carcinoma.

Table I. Differential protein identification.

Sample ID	Protein	Protein ID no.	Functional characteristics of the protein (OMIM ID and chromosome location, if known)
Clear cell carcinoma			
C1	Annexin A2	4757756	A member of the annexin (lipocortin) family of calcium-dependent phospholipids and membrane-binding proteins; substrate of the SRC tyrosine kinase; possible autocrine factor (151740; 15q21-q22)
C2	Fibrinogen γ-A chain precursor	71827	A member of the fibrinogen family, which plays a role in the adhesion and aggregation of platelets (134850; 4q28)
C3	Annexin A4	1703319	A member of the annexin (lipocortin) family of proteins; has been suggested to play a role in regulation of water and protein permeability of cell membranes in an aquaporin-independent manner (106491; 2p13)
C4	Cathepsin D preprotein	4503143	A lysosomal aspartic proteinase involved in degredation of proteins, antigen processing, and involved in mediation of apoptosis; has been suggested to play a role in growth and metastatic potential of epithelial cancers, especially breast cancer (116840; 11p15.5)
C5	α enolase	2661039	An isoform of the glycolytic enzyme enolase, which is involved in basic energy and metabolism, as well as plasminogen binding and activation; wide-spread tissue distribution and expression in the early stages of embryonic development (607098; N/A)
C6	Proteasome activator subunit 1	5453990	Activates multicatalytic protease, which degrades protein conjugated to ubiquitin; up-regulated by interferon γ (600654; 14q11.2)
C7	Glutathione transferase ω	4758484	Acts as a stress response protein involved in cellular redox homeostasis (N/A)
C8	Tubulin, ß2	5174735	Member of the tubulin family; component of microtubules which are critical for cell division and proper segregation of chromosomes, abnormal function leads to aneuploidy (602660; N/A)
Papillary carcinoma			
P1	NADH dehydrogenase FeS protein	227297	Involved in the electron transport chain of mitochondrial oxidative phosphorylation (N/A)
P2	Dihydrolipoamide succinyltransferase	643589	Member of a multienzyme complex within the mitochondrion involved in catalyzing oxidative decarboxylation of α-keto acids (126063; 14q24.3)
P3	Annexin A2	18645167	A member of the annexin (lipocortin) family of calcium-dependent phospholipids and membrane-binding proteins; substrate of the SRC tyrosine kinase; possible autocrine factor (151740; 15q21-q22)
P4	Phosphotriesterase-related gene	20070186	A zinc metalloenzyme catalyzing the hydrolysis of phosphotriester compounds; expressed in normal renal tubules (604446; 10p12)
P5	Annexin I	4502101	A member of the annexin (lipocortin) family; anti-inflammatory action of glucocorticoids attributed to annexin's inhibition of phospholipase A2; found in renal medullary cells (151690; 9q11-q22)
P6	Capping protein, actin filament, gelsolin-like	4502561	A member of the gelsolin family of proteins that caps actin filament ends in non-muscle cells to help alter shape during movement; found in renal tubular cells (153615; 2cen-q24)
P7	Lamin A precursor	34228	One of 3 known members of lamin family; nuclear lamina proteins which are associated with rare forms of muscular dystrophy, lipodystrophy, and familial dilated cardiomyopathy (150330; 1q21.2)
P8	γ enolase	693933	A member of the enolase family of glycolytic pathway enzymes; major form of enolases found in neurons (131360; 12p13)
P9	ß actin	4501885	The major form of non-muscle cytoskeletal actin (102630; 7p220p12)
P10	α tubulin	32015	Alternatively spliced α-tubulin, preferentially expressed in testis; interacts to form microtubules (191110; 2q)

Table I. Continued.

Sample ID	Protein	Protein ID no.	Functional characteristics of the protein (OMIM ID and chromosome location, if known)
Wilms' tumor			
W1	Ariadne-2 protein homolog	18202259	RING finger (specialized zinc finger domain), upregulated during retinoic acid-induced granulocytic differentiation of acute promyelocytic leukemia cells (605615; chromosome 3)
W2	Zinc finger protein 267	604752	Zinc finger protein (604752; chromosome 16)
W3	Makorin 1	17369682	Source for a family of genes encoding a novel class of zinc finger proteins (607754; N/A)
W4	Krueppel-related zinc finger protein (zinc finger 184)	33302618	Zinc finger protein (602277; 6p21.3)
W5	Golgi-apparatus protein 1 precursor	17376711	A membrane sialoglycoprotein residing in the medial cisternae of the Golgi apparatus of most cells; thought to play an important role in the biogenesis and function of the Golgi apparatus; highly homologous to ESL-1, a ligand for E-selectin (600753; 16q22-q23)
Oncocytoma			
O1	Metallothionein-1A	127365	A metal-binding protein, thought to detoxify metals (zinc, copper), to control metal levels during development, and to protect against oxidative stress (156350; 16q13)
O2	Antioxidant protein 1 (ATOX1)	602270	Critical role in copper homeostasis; usually located in the renal cortex and the medullary loop of Henle; may also play a role in anti-oxidant defense (602270; 5q32)
O3	Metallothionein-1L	462637	Member of metallothionein family of low molecular weight; heavy metal-binding proteins (156358; 16q13)
O4	Pyruvate dehydrogenase E1 component, ß	129070	A member of the multi-subunit pyruvate dehydrogenase family involved in intermediate metabolism (N/A)

Protein ID no., protein identification number in the NCBI database (http://www.ncbi.nlm.nih.gov). OMIM, Online Mendelian Inheritance in Man (http://www.ncbi.nlm.nih.gov). Additional references on protein function and role in health and disease can be found in the OMIM online database, with cross-references to citations available in PubMed (http://www.ncbi.nlm.nih.gov). Gene location refers to human chromosome location, if known. N/A, not available.

differentially-expressed spots, each of which contains a 'purified' accumulation of the same protein. The protein sequence was identified after spectrometric analysis of two or more peptide sequences whose probability scores met or exceeded the threshold for statistical significance ($p<0.05$).

Four to nine differentially-expressed, randomly-selected protein spots per tumor type were analyzed by mass spectrometry to document the utility of this approach. Therefore, the list of identified proteins is incomplete. Also, the analyzed proteins were identified within the pH 4.0-7.0 range that was chosen for this study. Nevertheless, the list of differentially expressed and sequenced proteins (Table I) revealed distinct protein spectra that may further elucidate the histogenetic, functional, and metabolic characteristics of the individual groups of tumors under study. Proteomic analysis of papillary carcinomas, which may represent the most differentiated of the four investigated tumor types, revealed a significant number of structural proteins or proteins that are also found in normal kidney (P3, P4, P5, P7, P9, P10). In contrast, the examination of clear cell carcinoma revealed less organ-specific regulatory proteins (C1, C3, C4, C5, C6, C7), including α-enolase, which is widely distributed during early stages of embryonic development. Four out of five proteins sequenced from embryonal Wilms' tumor tissue revealed proteins with zinc finger domains (W1, W2, W3, W4), suggestive of nuclear transcription activity. Two proteins detected in renal oncocytoma belong to the metallothionein family (O1, O3), which may be related to the abundant mitochondria seen in these tumors.

Further experiments are in progress to identify additional, differentially-expressed proteins and to characterize their function. We conclude that the described approach is valuable, sensitive and a specific translation of morphological phenotype into a corresponding proteotype. Subsequent

protein identification by MS is highly specific and is expected to be a substantial support for biomarker discovery in the future.

Acknowledgements

We would like to thank The Gerber Foundation, Hauenstein Foundation, The Fischer Family Trust, and Schregardus Family Foundation for their ongoing support of the Van Andel Research Institute kidney cancer program. We thank the Cooperative Human Tissue Network of National Cancer Institute (CHTN) for providing the renal tumor samples. We would also like to thank Sabrina Antio for manuscript preparation and submission.

References

1. Petricoin EF, Ardekani AM, Hitt BA, *et al*: Use of proteomic patterns in serum to identify ovarian cancer. Lancet 359: 572-577, 2002.
2. Adam BL, Qu Y, Davis JW, *et al*: Serum protein fingerprinting coupled with a pattern-matching algorithm distinguishes prostate cancer from benign prostate hyperplasia and healthy men. Cancer Res 63: 3609-3614, 2002.
3. Bergquist J, Palmblad M, Wetterhall M, Hakansson P and Markides KE: Peptide mapping of proteins in human body fluids using electrospray ionization Fourier transform ion cyclotron resonance mass spectrometry. Mass Spectrometry Rev 21: 2-15, 2002.
4. Vlahou A, Schellhammer PF, Mendrinos S, *et al*: Development of a novel proteomic approach for the detection of transitional cell carcinoma of the bladder in urine. Am J Pathol 158: 1491-1502, 2001.
5. Pang JX, Ginanni N, Dongre AR, Hefta SA and Opitek GJ: Biomarker discovery in urine by proteomics. J Proteome Res 1: 161-169, 2002.
6. Yao Y, Berg EA, Costello CE, Troxler RF and Oppenheim FG: Identification of protein components in human acquired enamel pellicle and whole saliva using novel proteomics approaches. J Biol Chem 278: 5300-5308, 2003.
7. Craven RA, Totty N, Harnden P, Selby PJ and Banks RE: Laser capture microdissection and two-dimensional polyacrylamide gel electrophoresis: evaluation of tissue preparation and sample limitations. Am J Pathol 160: 815-822, 2002.
8. Craven RA and Banks RE: Use of laser capture microdissection to selectively obtain distinct populations of cells for proteomic analysis. Methods Enzymol 356: 33-49, 2002.
9. Schwartz SA, Reyzer ML and Caprioli RM: Direct tissue analysis using matrix-assisted laser desorption/ionization mass spectrometry: practical aspects of sample preparation. J Mass Spectrom 38: 699-708, 2003.
10. Storkel S, Eble JN, Adlakha K, *et al*: Classification of renal cell carcinoma: Workgroup No. 1. Union Internationale Contre le Cancer (UICC) and the American Joint Committee on Cancer (AJCC). Cancer 80: 987-989, 1997.
11. Goelz SE, Hamilton SR and Vogelstein B: Purification of DNA from formaldehyde fixed and paraffin embedded human tissue. Biochem Biophys Res Commun 130: 118-126, 1985.
12. Bhattacharya SH, Gal AA and Murray K: Laser capture microdissection MALDI for direct analysis of archival tissue. J Proteome Res 2: 95-98, 2003.
13. Palmer-Toy DE, Sarracino DA, Sgroi D, Le Vangie R and Leopold PE: Direct acquisition of matrix-assisted laser desorption/ionization time-of-flight mass spectra from laser capture microdissected tissues. Clin Chem 46: 1513-1516, 2000.
14. Chaurand P, Schwartz SA, Billheimer D, Xu BJ, Crecelius A and Caprioli RM: Integrating histology and imaging mass spectrometry. Anal Chem 76: 1145-1155, 2004.
15. Gottlieb M and Chavko M: Silver staining of native and denatured eucaryotic DNA in agarose gels. Anal Biochem 165: 33-37, 1987.
16. Blum H, Beier H and Gross HJ: Improved silver staining of plant-proteins, RNA and DNA in polyacrylamide gels. Electrophoresis 8: 93-99, 1987.
17. Stone KL and Williams KR: Enzymatic digestion of proteins and HPLC peptide isolation. In: A Practical Guide to Protein and Peptide Purification for Microsequencing. Matsudaira P (ed). Academic Press, San Diego, 1993.
18. Perkins DN, Pappin DJC, Creasy DM and Cotrell JS: Probability-based protein identification by searching sequence databases using mass spectrometry data. Electrophoresis 20: 3551-3567, 1999.
19. Boeckmann B, Bairoch A, Apweiler R, *et al*: The SWISS-PROT protein knowledgebase and its supplement TrEMBL in 2003. Nucleic Acids Res 31: 365-370, 2003.
20. Moore RE, Young MK and Lee TD: Qscore: An algorythm for evaluating SEQUEST database search results. J Am Soc Mass Spectrom 13: 378-386, 2002.